

# Reducing decoherence of the confined exciton state in a quantum dot by pulse-sequence control

V. M. Axt,<sup>1</sup> P. Machnikowski,<sup>1,2,\*</sup> and T. Kuhn<sup>1</sup>

<sup>1</sup>*Institut für Festkörperteorie, Westfälische Wilhelms-Universität, 48149 Münster, Germany*

<sup>2</sup>*Institute of Physics, Wrocław University of Technology, 50-370 Wrocław, Poland*

We study the phonon-induced dephasing of the exciton state in a quantum dot excited by a sequence of ultra-short pulses. We show that the multiple-pulse control leads to a considerable improvement of the coherence of the optically excited state. For a fixed control time window, the optimized pulsed control often leads to a higher degree of coherence than the control by a smooth single Gaussian pulse. The reduction of dephasing is considerable already for 2-3 pulses.

## I. INTRODUCTION

Modern semiconductor technology offers a range of ways to produce artificial systems where a small number of charges, confined in all three spatial dimensions, form atomic-like systems. These quantum dots<sup>1,2</sup> (QDs) allow one to optically control the quantum states in a way typical for atomic systems<sup>3,4,5,6,7,8,9,10</sup>, but they are still semiconductor charge devices, opening the possibility of integration into future nanoelectronic and quantum electronic devices<sup>11,12</sup>.

The recent progress in ultrafast spectroscopy of semiconductor systems<sup>13</sup> made it possible to control and probe the quantum states of carriers confined in a QD on femtosecond time scales. However, any interaction of the confined carriers with the external driving fields not only leads to the desired quantum transitions but also can induce some unwanted ones. If both the desired and unwanted transitions have a discrete nature (e.g., the exciton vs. biexciton transition in a QD) the latter may be suppressed by a suitable choice of control pulses<sup>14,15</sup>. However, since the QDs are embedded in the macroscopic crystal, an important role is played here by phonon-assisted transitions which inherit the continuous nature from the phonon states. The presence of a continuum in the system state obtained after optical excitation leads to irreversibility of the subsequent kinetics and to dephasing of the quantum states<sup>16,17,18,19,20</sup> even in the absence of real transitions (energy relaxation). In the latter case these processes are known as pure dephasing.

Effects of pure dephasing may be observed in measurements of the optical polarization<sup>17,18,19</sup> or exciton occupation in a QD<sup>18,21,22</sup>. The qualitative agreement between theoretical predictions based on the phonon-induced pure dephasing model<sup>19</sup> and four-wave-mixing data<sup>23</sup> confirms that these phonon-related processes dominate the dephasing in the sub-picosecond resonant driving regime. Recently, it has been shown that the initial decoherence in QDs with strong electronic confinement as described by the pure dephasing model is also in quantitative agreement with corresponding measurements<sup>24</sup>. It turns out that even at low temperatures ( $\sim 5$  K) typically about 20 % of the coherence is lost already in the initial phase of the dynamics within a few picoseconds. Obviously, this rapid decoherence is

not negligible and can potentially become an obstacle for many proposed device applications<sup>25,26</sup>.

The question arises whether it is possible to reduce the phonon-assisted component of the final state by some pulse shaping techniques, e.g., by using sequences of pulses, in analogy to the discrete transition case<sup>14,15</sup>. It is clear that the continuum nature of these unwanted transitions makes this task much more demanding. One obvious way of excluding the phonon-assisted transitions is to make the control pulse spectrally selective by extending the pulse durations. This is, however, disadvantageous when other decoherence processes are present that decrease the coherence properties of the final state if the control operation takes too long and lead to a trade-off situation<sup>27</sup>. For practical purposes it is therefore essential to minimize the phonon-related pure dephasing with the constraint that the time window for the control action is limited.

In this paper we propose a solution to this optimization problem in terms of a control sequence composed of a series of ultrashort (but finite) pulses. The advantage of this approach is that it is simple both in theoretical formulation and experimental realization, as it does not require the technical ability to obtain arbitrary pulse shapes. Moreover, sequences of temporally broadened pulses have simple spectral features, even in the nonlinear regime, which lead to a transparent interpretation of the resulting dephasing effect.

On the other hand, in spite of the apparently limited class of pulse shapes considered, the proposed approach turns out to be unexpectedly efficient. Already for a few pulses the degree of decoherence falls down considerably, while a further increase of the pulse number leads only to negligible improvement. We shall show also that achieving by a single Gaussian pulse the same dephasing as that resulting from a sequence of a few pulses often requires much longer control times. Thus, the quality of coherent optical control of the excitonic system can indeed be increased by simple means, using series of phase-locked laser pulses, without the need to generate pulses of arbitrary shape.

The paper is organized as follows. In the next section we present the model of the carrier-phonon system. In Sec. III we discuss the limiting case of infinitely short pulses which can be treated analytically. In order to

demonstrate the reduction of decoherence by multiple-pulse control we compare the coherence losses occurring after a single pulse excitation with a given pulse area with those occurring after a pulse sequence with the same total pulse area. Next, in Sec. IV, we present a perturbative method for determining the coherence loss for arbitrarily shaped pulses and apply it to the case of multiple-pulse sequences. The loss of coherence after a series of driving pulses with fixed finite pulse durations and optimized intensities is discussed in Sec. V. Physically, the duration of the pulses is limited to the lower end by the requirement to spectrally avoid higher energetic excitations which would be a source of further undesired dynamics and which are not accounted for in our model. In Sec. VI we extend our material model and subsequently include LO phonons and higher excited electronic states. Explicitly including these excitations in our optimization procedure allows us to use shorter pulses as building blocks of our pulse sequences. The undesired dynamics resulting from excitations of these higher energetic states is now avoided by optimizing the pulse sequence. Finally Sec. VII concludes the paper.

## II. THE MODEL

The environment-induced process of loosing the phase relations between different components of quantum superpositions may be observed experimentally in a number of ways. One of its manifestations is the decay of the optical polarization excited by a certain laser pulse or pulse sequence resonantly coupled to the ground-state excitonic transition in a quantum dot. The impact of this dephasing process was studied in the case of linear<sup>16,17</sup> and nonlinear<sup>18,19</sup> optical experiments.

Here, we consider the usual model of carrier-phonon interaction involving the two states of the carrier subsystem: the empty dot,  $|0\rangle$ , and the one exciton state,  $|1\rangle$ , the latter being coupled to phonon modes. The wave functions will be modeled by anisotropic Gaussians. We assume a simple product (Hartree) form of the exciton wave function with the hole component shrunk in-plane due to Coulomb interactions (this is consistent with previous results that were obtained by full numerical diagonalization methods<sup>20</sup>).

Thus, in the rotating wave approximation, the Hamiltonian reads (in the rotating frame)

$$H = \frac{1}{2}f(t)(|0\rangle\langle 1| + |1\rangle\langle 0|) + |1\rangle\langle 1| \sum_{\mathbf{k}} F_{\mathbf{k}}(b_{\mathbf{k}} + b_{-\mathbf{k}}^\dagger), \quad (1)$$

where  $f(t)$  is the pulse envelope (which will be assumed real),  $b_{\mathbf{k}}$  are the phonon annihilation operators for the mode  $\mathbf{k}$  (including implicitly also the branch index) and  $F_{\mathbf{k}}$  are phonon coupling constants for the ground exciton state. In the present paper the deformation potential coupling to the longitudinal acoustical (LA) phonons and the Fröhlich coupling to the longitudinal optical (LO)

Effective dielectric constant	$\tilde{\epsilon}$	62.6
Longitudinal sound speed	$c_l$	5600 m/s
LO phonon frequency	$\Omega$	54 ps <sup>-1</sup>
Deformation potential		
electrons	$\sigma_e$	-8.0 eV
holes	$\sigma_h$	1.0 eV
Crystal density	$\rho$	5360 kg/m <sup>3</sup>
Wave function widths:		
electron in-plane	$l_e$	4.4 nm
hole in-plane	$l_h$	3.6 nm
electron/hole in $z$ -direction	$l_z$	1.0 nm

TABLE I: The GaAs material parameters and QD system parameters used in the calculations (partly after Refs. 29,30).

phonons will be considered, with the corresponding coupling constants given by<sup>28</sup>

$$F_{\mathbf{k}} = \sqrt{\frac{\hbar k}{2\rho v c_l}} [\sigma_e \mathcal{F}_e(\mathbf{k}) - \sigma_h \mathcal{F}_h(\mathbf{k})] \quad (\text{LA}), \quad (2)$$

and

$$F_{\mathbf{k}} = -\frac{e}{k} \sqrt{\frac{\hbar \Omega}{2v \epsilon_0 \tilde{\epsilon}}} [\mathcal{F}_e(\mathbf{k}) - \mathcal{F}_h(\mathbf{k})] \quad (\text{LO}), \quad (3)$$

where  $\rho$  is the crystal density,  $c_l$  is the longitudinal sound speed,  $v$  is the normalization volume of the phonon modes,  $e$  is the elementary charge,  $\epsilon_0$  is the vacuum dielectric constant,  $\tilde{\epsilon} = (1/\epsilon_\infty - 1/\epsilon_s)^{-1}$  is the effective dielectric constant, where  $\epsilon_s$  and  $\epsilon_\infty$  are the static and high-frequency dielectric constants, respectively,  $\Omega$  is the LO phonon frequency and

$$\mathcal{F}_{e,h}(\mathbf{k}) = \int d^3r \Psi_{e,h}^*(\mathbf{r}) e^{i\mathbf{k}\cdot\mathbf{r}} \Psi_{e,h}(\mathbf{r}),$$

where  $\Psi_{e,h}(\mathbf{r})$  are the electron and hole wave functions. Since the electron and hole are assumed to overlap, the piezoelectric coupling will be neglected<sup>17</sup>. The parameters used in the computations are shown in Tab. I.

## III. POLARIZATION DEPHASING AFTER A SEQUENCE OF ULTRASHORT PULSES

The natural starting point for the discussion of the multiple-pulse control of the optical polarization in a QD seems to be the limit of ultrashort pulses. In this case, each pulse in the sequence acts on a time scale much shorter than the lattice response times. The subsequent evolution corresponds to a relaxation of the lattice to a new equilibrium that is determined by the optically created confined charge distribution. During this process the exciton occupation cannot change but the carrier-phonon correlations that appear in the system partly destroy the exciton coherence. The resulting decay of the

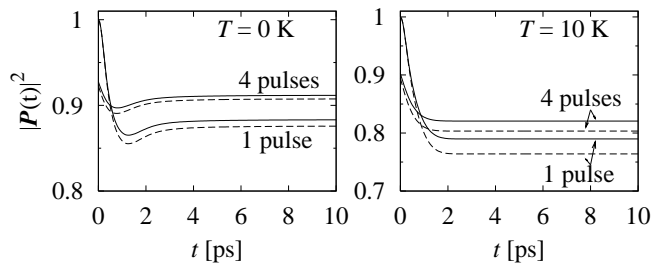


FIG. 1: The evolution of the optical polarization excited with one or four infinitely short pulses. Solid: exact result, dashed: perturbative result.

optical polarization may be described analytically, both for a single pulse<sup>17</sup> and for a sequence of pulses<sup>18</sup>.

It has been shown experimentally<sup>23,31</sup> that the optical polarization excited by an ultra-short pulse undergoes an initial dephasing on a picosecond time scale, followed by a much slower exponential decay. Model calculations reveal that the initial decay in these systems can be mostly attributed to LA phonons<sup>19,24</sup>. In general, decoherence refers to the loss of definite phase relations between various components of a quantum superposition. In our case these components are the crystal ground state and the QD exciton state. Most easily affected by decoherence is the superposition state with equal amplitudes, which is reached from the ground state by an  $\alpha = \pi/2$  rotation on the Bloch sphere. In the following we will concentrate on minimizing the decoherence occurring after such a  $\pi/2$  rotation. Other optimization goals have been considered and treated with other strategies<sup>32</sup>.

Analytical results for LA phonon-induced pure dephasing obtained along the lines described in Ref. 18 are plotted in Fig. 1. Shown is the evolution after a single  $\pi/2$  pulse and after a series of four identical, in-phase, equidistant  $\pi/8$  pulses. The total length of the series is  $t_{\text{tot}} = 1$  ps and the last pulse arrives at  $t = 0$ . The spectral cut-off resulting in real experiments from the finite pulse duration is introduced in this  $\delta$ -pulse model by including only the acoustic phonon response, which amounts to the assumption that the actual pulse duration is still longer than LO phonon periods and also long enough to spectrally avoid higher excitations.

Compared to the single-pulse excitation, the initial polarization in the 4-pulse case is reduced due to dephasing in between the pulses. However, the final level of polarization is higher. This means that the multiple-pulse excitation leads to a lower contribution of the phonon-assisted transitions in the final state. At zero temperature the loss of coherence compared to the single-pulse initial value is reduced from about 12% to about 9%, i.e., we obtain an improvement of 25%. In the remaining part of the paper we will explore the possibilities of reducing the degree of dephasing, going beyond the  $\delta$ -pulse limit and, finally, extending the modeling to higher-energetic excitations.

#### IV. PHONON-INDUCED PERTURBATION OF THE COHERENT DYNAMICS

It may be expected that the reduction of dephasing described in the previous Section may be extended by increasing the number of pulses and optimizing their amplitudes. However, the analytical formulas become highly involved for growing numbers of pulses. In any case the spectral width of a sequence of  $\delta$  pulses will be infinite (although, possibly, the spectra may get non-trivially shaped). Here, it should be recalled that the spectral selectivity of real experiments has been accounted for in this approach by concentrating on the lattice response in the low-frequency regime and disregarding in the material model all higher energetic excitations. A more accurate treatment of the spectral selectivity is, of course, to introduce a spectral cut-off. This requires using finite-length pulses; a case for which within our model no exact solution of the dynamics is known.

In order to deal with these issues and to continue and extend our discussion without restricting it to linear optical effects we resort to a scheme which is non-perturbative in the electromagnetic field but includes the phonon effects only in the leading order.

To calculate the phonon-related perturbation we expand the formal expression for the density matrix of the total system (in the interaction picture) at the final time  $t$  up to the second order in the phonon coupling constants<sup>33</sup>.

$$\begin{aligned} \tilde{\varrho}(t) = & \tilde{\varrho}(t_i) + \frac{1}{i\hbar} \int_{t_i}^t d\tau [H_{\text{int}}(\tau), \varrho(t_i)] \\ & - \frac{1}{\hbar^2} \int_{t_i}^t d\tau \int_{t_i}^{\tau} d\tau' [H_{\text{int}}(\tau), [H_{\text{int}}(\tau'), \varrho(t_i)]], \end{aligned} \quad (4)$$

where  $\tilde{\varrho}(t)$  and  $H_{\text{int}}(\tau)$  are, respectively, the density matrix of the total system and the carrier-phonon interaction Hamiltonian in the interaction picture with respect to the laser-induced evolution (which, in the case of resonant coupling, is known exactly) and  $t_i$  is the initial time. We assume an uncorrelated initial state with the lattice in thermal equilibrium and the exciton subsystem in the ground state. This procedure does not involve any Markovian approximations; the truncation at the second order is valid as long as the correction to the density matrix remains small.

After tracing out the lattice degrees of freedom and setting  $\alpha = \pi/2$  the polarization at the time  $t$ , which is proportional to  $\varrho_{01}(t)$ , may be written as

$$|P(t)|^2 = |P_0|^2 \left[ 1 - \int d\omega \frac{R(\omega)}{\omega^2} |K(\omega) - e^{i\omega t}|^2 \right], \quad (5)$$

where

$$K(\omega) = \int_{-\infty}^{\infty} d\tau e^{i\omega\tau} \frac{d}{d\tau} \sin \Phi(\tau), \quad (6)$$

$$\Phi(\tau) = \int_{-\infty}^{\tau} d\tau' f(\tau').$$

The upper limit of integration in Eq. (6) has been extended to infinity under the assumption that at time  $t$  the pulse has already been completely switched off (the details of the formalism are described in Ref. 34). Since the function  $R(\omega)/\omega^2$  is regular at  $\omega = 0$ , the asymptotic limit of the polarization at  $t \rightarrow \infty$  is (cf. Ref. 17)

$$|P(\infty)|^2 = |P_0|^2 \left[ 1 - \int d\omega \frac{R(\omega)}{\omega^2} (|K(\omega)|^2 + 1) \right]. \quad (7)$$

The phonon spectral densities  $R(\omega)$  characterize the spectral properties of the lattice and are given by

$$R(\omega) = \frac{1}{\hbar^2} |n_B(\omega) + 1| \times \sum_{\mathbf{k}} |F_{\mathbf{k}}|^2 [\delta(\omega - \omega_{\mathbf{k}}) + \delta(\omega + \omega_{\mathbf{k}})], \quad (8)$$

where  $n_B(\omega)$  is the Bose distribution function.

It should be noted that part of the polarization drop can be attributed to the deformation polaron formation around the exciton (phonon dressing) which is not necessarily irreversible. In fact, a perfectly adiabatic, thus reversible, passage to the exciton-no-exciton superposition corresponds to vanishing  $K(\omega)$  and, although no irreversible dynamics takes place, there is still a relative polarization reduction

$$\delta_\infty = \int d\omega \frac{R(\omega)}{\omega^2},$$

which corresponds to 1/2 of the asymptotic value after a  $\delta$  pulse.

Since the spectral function  $K(\omega)$  [Eq. (6)] is a nonlinear functional of the pulse envelope  $f(t)$ , the only way of calculating it is, in general, to numerically perform the Fourier integral. However, some insight in its structure is possible in the case of a series of non-overlapping control pulses. Let us denote the  $n$ th pulse envelope ( $n = 1, \dots, N$ ) by  $f_n(t - t_n)$ , where  $t_n$  is the time at which the pulse is applied, and the value of  $\Phi(t)$  after the  $n$ th pulse by  $\alpha_n$ , with  $\alpha_0 = 0$  and  $\alpha_N \equiv \alpha$ . Then, during the  $n$ th pulse one has

$$\Phi(\tau) = \alpha_{n-1} + \tilde{\Phi}_n(\tau - t_n),$$

where

$$\tilde{\Phi}_n(\tau) = \int_{-\infty}^{\tau} f_n(\tau') d\tau'.$$

Substituting this into Eq. (6) one finds

$$K(\omega) = \frac{1}{2i} [F(\omega) - F^*(-\omega)], \quad (9)$$

$$F(\omega) = \sum_{n=1}^N \tilde{F}_n(\omega) e^{i(\alpha_{n-1} + \omega t_n)}, \quad (10)$$

with

$$\tilde{F}_n(\omega) = \int dt e^{i\omega t} \frac{d}{dt} e^{i\tilde{\Phi}_n(t)},$$

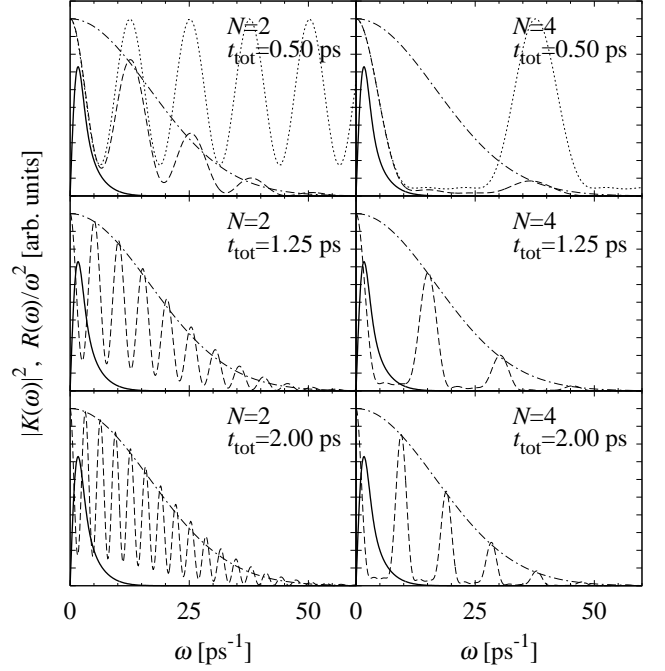


FIG. 2: Spectral characteristics of the phonon reservoir and of the driven dynamics. Solid line: The spectral density  $R(\omega)/\omega^2$  at  $T = 0$  K for LA phonons. Dashed line: the nonlinear spectrum  $|K(\omega)|^2$  for a sequence of identical short pulses for  $\alpha = \pi/2$  and pulse numbers and total durations as shown. Dash-dotted line: the envelope calculated as the linear spectrum of a single pulse (up to an appropriate factor). In the upper figures also the nonlinear spectrum for a sequence of  $\delta$ -pulses is shown (dotted).

Since, by definition, the function  $\tilde{\Phi}_n(t)$  changes only around  $t = 0$ , the transform  $\tilde{F}_n(\omega)$  is a smooth envelope of width inversely proportional to the duration of the pulse  $f_n(t)$ . If the rotation angle per pulse is small this envelope function is close to the linear Fourier transform of  $f_n(t)$  (up to a factor).

In the limit of infinitely short pulses the transform  $\tilde{F}_n(\omega)$  becomes infinitely broad and one has

$$\tilde{F}_n(\omega) = \tilde{F}_n(0) = e^{i(\alpha_n - \alpha_{n-1})} - 1. \quad (11)$$

If, in addition, the pulses are equally spaced,  $t_n = n\Delta t$ , then the resulting spectral function  $F(\omega)$  is periodic in the frequency domain with the period  $2\pi/\Delta t$ . This limit corresponds to the exact solution obtained previously and allows one to compare both results and estimate the error introduced by the perturbative approach. As can be seen in Fig. 1, the perturbative results not only reproduce qualitatively all the essential features of the exact result but are also reasonably close to the exact results, at least at low temperatures.

Temporally broadening the pulses results in the appearance of the envelopes  $\tilde{F}_n(\omega)$  [Eq. (10)] which break the periodicity and eliminate the high-frequency part of the nonlinear spectrum. For a series of identical, weakly

overlapping, equally spaced pulses one has  $\tilde{F}_n(\omega) \equiv \tilde{F}(\omega)$ ,  $\alpha_n = n\alpha/N$ , and  $t_n = (n-1)\tilde{T}/N$ . In order to simplify the formulas, we define here  $\tilde{T} = Nt_{\text{tot}}/(N-1)$ , where  $t_{\text{tot}}$  is the total length of the pulse sequence measured from the center of the first pulse to the center of the last. The summation in Eq. (10) may be easily performed analytically and the result for  $\alpha = \pi/2$  is

$$|K(\omega)|^2 = \frac{1}{4} |\tilde{F}(\omega)|^2 \left[ \frac{\sin^2 \frac{\tilde{T}}{2}(\omega + \frac{\pi}{2\tilde{T}})}{\sin^2 \frac{\tilde{T}}{2N}(\omega + \frac{\pi}{2\tilde{T}})} + \frac{\sin^2 \frac{\tilde{T}}{2}(\omega - \frac{\pi}{2\tilde{T}})}{\sin^2 \frac{\tilde{T}}{2N}(\omega - \frac{\pi}{2\tilde{T}})} \right]. \quad (12)$$

This is formally identical to the sum of two diffraction patterns for equally spaced optical grids of length  $\tilde{T}$ , modulated by the envelope  $\tilde{F}(\omega)$  which suppresses higher order “diffraction maxima”, and shifted oppositely by  $\pm\pi/(2\tilde{T})$ . This behavior is illustrated in Fig. 2, where we have chosen pulses with a duration of  $\tau_p = 100$  fs (full width at half maximum, FWHM). As seen in the figure, this choice assures that the relevant spectral function  $|K(\omega)|^2$  has a spectral cutoff below the LO phonon frequency  $\Omega = 54 \text{ ps}^{-1}$ , consistent with the neglect of this excitation in our model.

In this case of identical, weakly overlapping, equally spaced pulses, for increasing pulse number the period of the spectrum in the frequency domain increases, i.e. the higher maxima are shifted towards higher frequency and decrease due to the envelope. However, the width of the central maximum is determined by the total duration of the sequence. From Eq. (12) it can be seen that when taking  $\tilde{T}$  as a measure of the sequence duration then this width is essentially insensitive to the pulse number. Similarly, the value at  $\omega = 0$  is fixed by the gate angle and is always  $|K(0)|^2 = \sin \alpha = 1$ . Modifying the total duration of the sequence leads to proportional scaling of the  $\omega$ -dependence of the nonlinear spectrum  $|K(\omega)|^2$  (the “diffraction pattern”) under the envelope. The latter is fully determined by the single pulse spectrum which, for  $\alpha \lesssim \pi/2$  is very close to the linear one even for two pulses (see Fig. 2).

The independent control over the nonlinear spectrum for high frequencies (by pulse width) and in the LA frequency domain (by the sequence length and pulse number) opens the possibility of optimizing the coherence by reducing the overlap in Eq. (7), alternative to using long smooth pulses. In the next Section we study this issue, releasing the restriction to equal pulses in order to find optimized pulse sequences.

## V. REDUCTION OF DEPHASING BY OPTIMIZED PULSE SEQUENCES

The aim of this Section is to quantify the reduction of the LA-phonon induced dephasing of the optical polarization by using optimized sequences of pulses with a fixed finite pulse length. As discussed in the previous

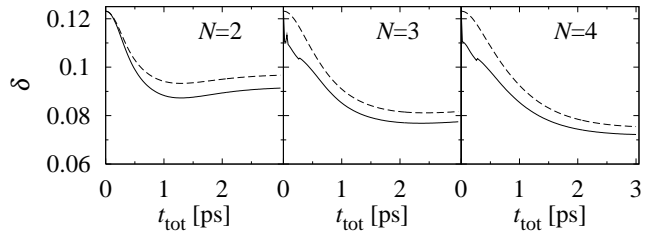


FIG. 3: The relative polarization drop (with respect to the unperturbed case) for the  $\alpha = \pi/2$  excitation performed by sequences of  $N = 2, 3, 4$  equidistant narrow pulses with  $\tau_p = 100$  fs within the time interval  $t_{\text{tot}}$  at  $T = 0$  K for optimized pulse intensities (solid) and for identical pulses (dashed).

Section, by using pulses of finite duration we impose an envelope on the nonlinear spectra of the controlled dynamics and thereby assure that higher-frequency spectral features, including LO phonons, higher exciton states and confined two-pair excitations, have negligible impact.

In real systems, apart from the pure dephasing resulting from the phonon response to the evolution of the exciton state there is another contribution to the loss of fidelity related to exponential decay processes (finite exciton lifetime in our specific case)<sup>23,35</sup>. The effect of the latter on the polarization magnitude grows with the duration of the pulse sequence. Therefore, a question of practical importance is to what extent the system coherence may be preserved against the pure dephasing during an operation performed by a sequence of a fixed number of pulses within a definite time interval that is limited by the exponential decoherence.

By numerically calculating the nonlinear spectra  $K(\omega)$  [Eq. (6)] for sequences of  $N$  equidistant narrow (but not necessarily non-overlapping) pulses and maximizing the asymptotic polarization magnitude [Eq. (7)] with respect to the pulse amplitudes for a fixed total rotation angle  $\alpha = \pi/2$  we found optimized<sup>38</sup> pulse sequences for a given total duration of the sequence  $t_{\text{tot}}$  and the resulting minimal polarization drop

$$\delta = \frac{|P_0|^2 - |P(\infty)|^2}{|P_0|^2}.$$

The result is shown in Fig. 3.

As expected, it turns out that the degree of dephasing typically tends to decrease as the time interval becomes longer. Optimizing the pulse sequence leads to some further reduction of the polarization drop compared to the case of equal pulses, although this additional gain is relatively small. An interesting feature is the slight increase of the decoherence drop for times  $t_{\text{tot}} \gtrsim 1$  ps in the  $N = 2$  case. This may be understood with the help of Fig. 2 by noting that for  $2\pi/t_{\text{tot}} \simeq \omega_{\text{LA}}$ , where  $\omega_{\text{LA}}$  is the LA spectral density cut-off, the maximum of  $R(\omega)/\omega^2$  coincides with the minimum of  $|K(\omega)|^2$  while for longer times the latter is quickly oscillating and averages to its mean value.

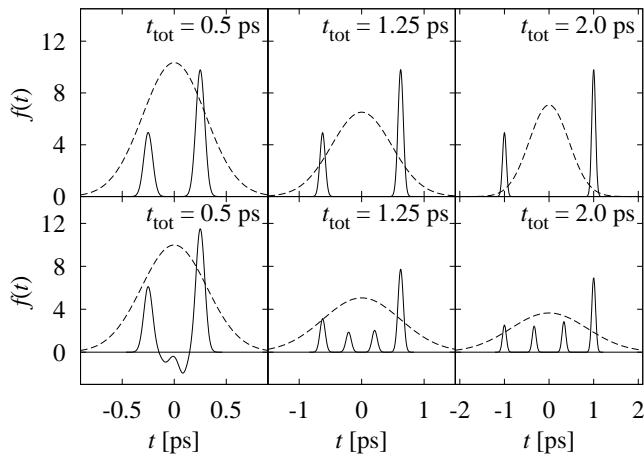


FIG. 4: The optimized sequences of  $N = 2$  (upper) and  $N = 4$  (lower) narrow pulses ( $\tau_p = 100$  fs) compared to the Gaussian pulses (dashed, arbitrary scale) yielding the same asymptotic polarization (at  $T = 0$  K).

For  $t_{\text{tot}} \lesssim \tau_p$  the duration of the pulse sequence is actually determined by  $\tau_p$  and  $t_{\text{tot}}/N$  becomes the shortest relevant time scale. Thus, the high frequency part of the pulse spectrum is governed by  $t_{\text{tot}}/N$  in this case and the simple discussion presented above for non-overlapping pulses is not valid. In this case, the nonlinear spectra extend to much larger frequencies and the overall error drops down due to strong modulations of the resulting pulse shape. Although the spectral cut-off cannot be assured *a priori* in this case, it is still possible to control the consistency of the calculation by inspection of the nonlinear spectrum corresponding to the resulting optimized pulse sequence. In fact, it turns out that for very short  $t_{\text{tot}}$  the error values shown in Fig. 3 do not correspond to pulse sequences with properly restricted spectra. Moreover, due to the very complex structure of the error as a function of the pulse intensities it is not guaranteed that the optimized value found by our procedure in the strong overlap regime corresponds to the global minimum. For weak and moderate overlap the optimized sequences are likely to correspond to the global minimum.

It is interesting to compare the coherence loss for an excitation performed by a sequence of pulses and by a single Gaussian pulse. In Fig. 4 we compare the optimized pulse sequence with a Gaussian pulse performing the same  $\alpha = \pi/2$  rotation with the same asymptotic polarization drop as obtained from the sequence. It turns out that already for  $N = 2$  the pulse sequence is shorter than the corresponding Gaussian pulse as long as  $t_{\text{tot}} \lesssim 2$  ps. For very short pulse durations the Gaussian may even be twice as long as the pulse sequence. For  $t_{\text{tot}} \gtrsim 2$  ps, the smooth Gaussian control can no longer be significantly outperformed by a pulse sequence. However, as the number of pulses is increased the pulsed control becomes more efficient over a wider range of sequence durations.

Another interesting aspect worthwhile to note is that

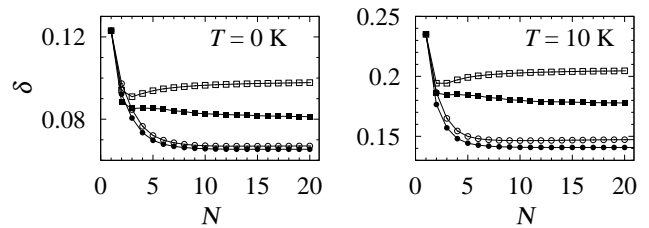


FIG. 5: The polarization drop as a function of the number of pulses  $N$  for the total durations  $t_{\text{tot}} = 1$  ps (squares) and  $t_{\text{tot}} = 5$  ps (circles) at  $T = 0$  K (left) and  $T = 10$  K (right). Full symbols: optimized pulse intensities, empty symbols: equal pulses. Here  $\tau_p = 100$  fs.

in the infinitely short pulse limit the optimal sequence of  $N = 2$  pulses does not depend on the structure of the spectral density of the reservoir and for  $\alpha = \pi/2$  it always corresponds to the ratio of pulse areas of 1:2 (see the Appendix). As can be seen in Fig. 4, this universal area ratio of the optimal 2-pulse sequence holds approximately also for pulses of finite duration.

By increasing the number of pulses, the coherence loss may be further reduced (Fig. 5). We find that at both temperatures the polarization drop can be reduced by about 40%. Note that even in the adiabatic limit, 50% of the polarization drop is present. This implies that the irreversible effect is reduced by about 80%. The reduction strongly depends on the total duration but in all cases (for  $t_{\text{tot}}$  in the picosecond range) most of it is gained already for a few pulses. For short  $t_{\text{tot}}$  and for a control sequence consisting of equal pulses there is an optimal number of pulses beyond which the error grows again. This results directly from Eq. (12): for higher  $N$  the nonlinear spectrum decreases more slowly around  $\omega = 0$  which determines the resulting overlap with  $R(\omega)$  when the width of the “zeroth order” maximum is comparable to the LA cut-off frequency. This effect disappears if one allows variable pulse intensities. From Fig. 5 it is evident that for sufficiently long total durations  $t_{\text{tot}}$  of the pulse sequence the polarization drop  $\delta$  comes close to its value in the adiabatic limit already when the sequence comprises only a few pulses. In this case, the optimization of the intensities yields only a marginal improvement as is seen from the curves corresponding to  $t_{\text{tot}} = 5$  ps in Fig. 5. In contrast, for pulse sequences of short duration  $t_{\text{tot}}$ ,  $\delta$  is well above its adiabatic value, but the improvement resulting from the intensity optimization is now substantial as illustrated by the  $t_{\text{tot}} = 1$  ps curves in Fig. 5.

In order to see most clearly how the optimization of overlapping pulses leads to a decrease of decoherence let us compare the spectral features corresponding to equal and optimized pulses in the case of strong overlap (Fig. 6). In the optimized case, a strong modulation of the resulting pulse envelope is possible which leads to considerable reduction of the nonlinear spectrum in the LA sector. Such a modulation produces, however,

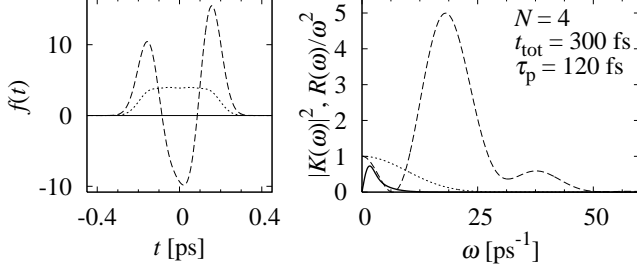


FIG. 6: Left: the optimized pulse envelope formed by the sequence of  $N = 4$  overlapping narrow pulses (dashed: pulses with optimized amplitudes, dotted: equal pulses) for the sequence duration  $t_{\text{tot}} = 0.3$  ps at  $T = 0$  K. Right: the corresponding nonlinear spectra  $|K(\omega)|^2$  along with the phonon spectral density (solid).

large spectral features beyond the LA cut-off, as can be clearly seen in Fig. 6. In order to provide the desirable spectral cutoff the pulse length must now be increased, compared to the case of non-overlapping pulses, or further constraints have to be introduced in the optimization procedure.

## VI. EXTENDING THE MODEL

As discussed above, the pulse lengths used to control the quantum state must be long enough to assure a frequency cut-off that avoids in any case the undesired dynamics that otherwise may result from high energetic excitations. This restriction may be inconvenient for practical applications as it implies the use of long pulses as building blocks of the control sequence. Below we show how the optimization procedure may be extended such that the undesired dynamics is not avoided by a frequency cut-off but rather by suitably shaping the pulse sequence. To this end we first need to extend our model and include explicitly the pertinent higher energetic excitations.

The first obvious step is to include LO phonons which, for confined states, contribute a single line (due to their weak dispersion around  $k = 0$ ). In the plot of the polarization drop against the duration (Fig. 7, left) small additional features appear periodically, both for equal as well as for optimized pulses (visible in the inset). They result from the fact that in the case of weakly overlapping pulses the positions of the maxima in the nonlinear spectrum  $|K(\omega)|^2$  are fixed by the total duration  $t_{\text{tot}}$  and the total number of pulses, and the decoherence effect increases each time one of them overlaps with the LO phonon line (Fig. 7, right). In the system under discussion this effect is rather weak because of the strong reduction of the LO phonon line due to charge cancellation. Note that extending the reservoir model allows us to reduce the pulse duration to 60 fs which now provides

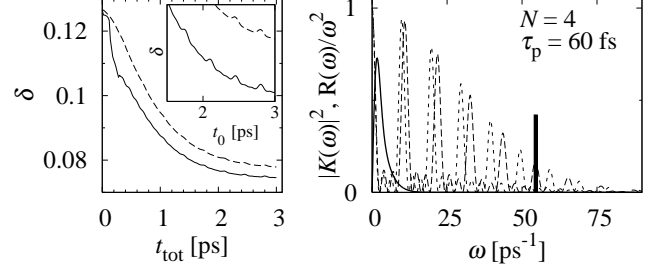


FIG. 7: Left: the asymptotic polarization decay induced by LA and LO phonons for  $N = 4$  pulses and  $\tau_p = 60$  fs; solid: optimized sequence, dashed: equal pulses. The inset shows part of the curves in magnification. Right: The nonlinear spectrum  $|K(\omega)|^2$  corresponding to two values of the pulse sequence duration  $t_{\text{tot}} = 1.74$  ps (strong overlap with the LO line; dashed) and  $t_{\text{tot}} = 1.92$  ps (weak overlap; dotted). Also shown are the spectral densities for LA (solid) and LO (bar, arbitrary scale) phonons.

the spectral cutoff before the onset of higher-frequency reservoir features.

The next higher excitations of the phonon bath are related to the possibility of phonon-assisted transitions to dark states<sup>36</sup> (which may be viewed as an effect of nonadiabaticity of exciton dynamics with respect to LO lattice oscillations<sup>37</sup>). We extend the Hamiltonian (1) by adding terms describing the excited exciton states and their LO-phonon-assisted coupling to the ground state (other couplings do not contribute to the leading order),

$$H_{\text{exc}} = \sum_{n>1} E_n |n\rangle\langle n| + \sum_{n>1} |1\rangle\langle n| \sum_{\mathbf{k}(\text{LO})} F_{\mathbf{k}}^{(n)} (b_{\mathbf{k}} + b_{-\mathbf{k}}^\dagger) + \text{H.c.},$$

where  $E_n$  are the energies of the excited states and the coupling constants  $F_{\mathbf{k}}^{(n)}$  are analogous to those given by Eqs. (2) and (3) and may be found e.g. in Ref. 20. This coupling induces additional decoherence with the corresponding asymptotic polarization drop given by

$$\Delta|P(\infty)|^2 = -|P_0|^2 \sum_{n>1} \int d\omega \frac{R^{(n)}(\omega - E_n)}{\omega^2} \left( |L(\omega)|^2 + \frac{1}{2} \right),$$

where

$$L(\omega) = \int_{-\infty}^{\infty} d\tau e^{i\omega\tau} \frac{d}{d\tau} \sin \frac{1}{2} \Phi(\tau), \quad (13)$$

and  $R^{(n)}(\omega)$  are defined as in Eq. (8) but with the coupling constants  $F_{\mathbf{k}}^{(n)}$  (see also Ref. 34). The optimal control, as measured by the minimal polarization drop, corresponds now to minimizing the sum of the overlap integral appearing in Eq. (7) and that given above.

For the results shown in Fig. 8, we include three optically inactive excited states at 17, 32 and 33 meV above

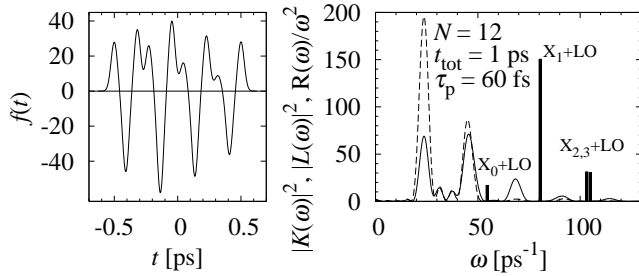


FIG. 8: The pulse sequence (left) and the nonlinear spectra (right) corresponding to the optimal control in the model extended by adding LO-phonon-assisted excitation of a few lowest dark states ( $X_1$ – $X_3$ ). In the right panel, the solid and dashed lines show the spectral functions  $|K(\omega)|^2$  and  $|L(\omega)|^2$ , respectively, while the vertical bars represent the spectral features related to phonon-assisted transitions to optically inactive states.

the ground state. The optimization was done for a relatively high number of pulses, so that they overlap giving rise to a single, strongly shaped envelope. The simple “diffraction pattern” argument does not hold in this case and strongly nonlinear effects become important. As a result, additional flexibility appears in the shaping of the nonlinear spectra and the pulse optimization leads to spectral functions that to a large extent avoid the overlap with these discrete transitions as can be seen in Fig. 8.

## VII. CONCLUSIONS

We have shown that the coherence of the optically generated superposition of exciton occupation states confined in a quantum dot may be considerably increased by using a sequence of narrow (but finite) pulses to drive the carrier system. By doing so, one modifies the nonlinear spectral properties of the optically driven evolution of the carrier subsystem which may decrease the overlap between these nonlinear spectra and the spectral features of the phonon reservoir.

Instead of expressing the admissible class of pulses in terms of mathematically defined constraints, the proposed approach relies on physically transparent semi-quantitative conditions. By using pulses of finite duration as building blocks one controls the frequency cut-off so that the spectra of the resulting pulses may be flexibly restricted to the frequency range of which one has reliable knowledge. In this way we guarantee that the result of the optimization is defined by the physical content of the carrier-phonon model and not by its unphysical truncations. On the other hand, by optimizing the pulse amplitudes the spectral properties of the resulting evolution are chosen in such a way that resonances with phonon modes are minimized.

Given a finite control time window, it is not possible to completely avoid the excitation of phonon modes and

the resulting dephasing of the exciton states (measurable via the decay of the optical polarization). This is due to the fact that the whole continuum of phonon frequencies cannot be avoided simultaneously. Nevertheless, with an optimized choice of pulse intensities the degree of dephasing may be considerably reduced, both at zero and finite temperatures, to a degree depending on the allowed duration of the pulse sequence (as expected, longer control time windows admit larger reduction of dephasing).

From the practical point of view, the results obtained in this paper are remarkable with two respects. First, in the picosecond range of control times (relevant for phonon-induced pure dephasing effects) using sequences of a few (2–4) pulses leads to higher final degree of coherence of the resulting state than that obtained by a single Gaussian pulse of the same total duration. This may be important since obtaining short series of phase-locked pulses is certainly much more feasible than generating an arbitrarily shaped pulse resulting from a full optimization procedure.

Second, it is found that increasing the pulse number beyond 3 or 4 brings only small improvements, compared to that gained by replacing the single pulse by a series of 2 or 3. This shows that the limited possibility of reducing the dephasing may be almost fully exploited already with limited control resources. The universality of the optimal sequence of two pulses further increases the usefulness of these results.

## Acknowledgments

We gratefully acknowledge the financial support for P.M. by the Alexander von Humboldt Stiftung. The work was partly supported by the Polish KBN Grant No. PB 2 PO3B 085 25.

## Appendix

### UNIVERSALLY OPTIMAL 2-PULSE SEQUENCE

In this appendix we show that the optimal amplitudes of two ultrashort pulses (in the limit of infinitely short pulses) depend only on the total rotation angle but not on the properties of the lattice reservoir.

Let us denote the total rotation angle by  $\alpha$  and the rotation angles performed by the first and second pulses (proportional to the corresponding pulse areas) by  $\alpha_1$  and  $\alpha_2 = \alpha - \alpha_1$ , respectively. Assuming the pulses to arrive at  $t = \pm t_{\text{tot}}/2$  and inserting Eq. (11) into Eqs. (10) and (9) one finds

$$|K(\omega)|^2 = \sin^2 \alpha + 2 \left( 1 - \cos \frac{\omega t_{\text{tot}}}{2} \right) (\sin^2 \alpha_1 - \sin \alpha \sin \alpha_1).$$



Since  $1 - \cos \omega t \geq 0$ , the minimum (with respect to  $\alpha_1$ ) of the overlap with the nonnegative function  $R(\omega)/\omega^2$  [Eq. (7)] always corresponds to the minimum of the rightmost bracket in the above formula. Therefore, irrespective of the specific form of  $R(\omega)$ , the optimal choice is

$$\sin \alpha_1 = \frac{1}{2} \sin \alpha.$$

For  $\alpha = \pi/2$  this corresponds to  $\alpha_1 = \pi/6$  and  $\alpha_2 = \pi/3$ , so that the pulse area ratio is 1:2. This result holds, however, only in the leading order in the phonon coupling and is no longer valid in the general, non-perturbative case.

- 
- \* Electronic address: Pawel.Machnikowski@pwr.wroc.pl
- <sup>1</sup> L. Jacak, P. Hawrylak, and A. Wojs, *Quantum Dots* (Springer Verlag, Berlin, 1998).
  - <sup>2</sup> U. Woggon, *Optical Properties of Semiconductor Quantum Dots* (Springer Verlag, Berlin, 1997).
  - <sup>3</sup> M. Bayer, O. Stern, P. Hawrylak, S. Fafard, and A. Forchel, *Nature* **405**, 923 (2000).
  - <sup>4</sup> A. Zrenner, E. Beham, S. Stuffer, F. Findeis, M. Bichler, and G. Abstreiter, *Nature* **418**, 612 (2002).
  - <sup>5</sup> N. N. Bonadeo, J. Erland, D. Gammon, D. S. Katzer, D. Park, and D. G. Steel, *Science* **282**, 1473 (1998).
  - <sup>6</sup> T. H. Stievater, X. Li, D. G. Steel, D. Gammon, D. S. Katzer, D. Park, C. Piermarocchi, and L. J. Sham, *Phys. Rev. Lett.* **87**, 133603 (2001).
  - <sup>7</sup> P. Borri, W. Langbein, S. Schneider, U. Woggon, R. L. Sellin, D. Ouyang, and D. Bimberg, *Phys. Rev. B* **66**, 081306 (2002).
  - <sup>8</sup> H. Kamada, H. Gotoh, J. Temmyo, T. Takagahara, and H. Ando, *Phys. Rev. Lett.* **87**, 246401 (2001).
  - <sup>9</sup> H. Htoon, T. Takagahara, D. Kulik, O. Baklenov, A. L. Holmes Jr., and C. K. Shih, *Phys. Rev. Lett.* **88**, 087401 (2002).
  - <sup>10</sup> X. Li, Y. W. D. Steel, D. Gammon, T. Stievater, D. Katzer, D. Park, C. Piermarocchi, and L. Sham, *Science* **301**, 809 (2003).
  - <sup>11</sup> D. Bimberg, M. Grundmann, and N. Ledentsov, *Quantum Dot Heterostructures* (Wiley, Chichester, 1999).
  - <sup>12</sup> L. Jacak, A. Wójs, and P. Machnikowski, in *Encyclopedia of Nanoscience and Nanotechnology*, edited by H. S. Nalwa (American Scientific Publishers, Stevenson Ranch, CA, 2004).
  - <sup>13</sup> V. M. Axt and T. Kuhn, *Rep. Prog. Phys.* **67**, 433 (2004).
  - <sup>14</sup> Pochung Chen, C. Piermarocchi, and L. J. Sham, *Phys. Rev. Lett.* **87**, 067401 (2001).
  - <sup>15</sup> C. Piermarocchi, Pochung Chen, Y. S. Dale, and L. J. Sham, *Phys. Rev. B* **65**, 075307 (2002).
  - <sup>16</sup> L. Besombes, K. Kheng, L. Marsal, and H. Mariette, *Phys. Rev. B* **63**, 155307 (2001).
  - <sup>17</sup> B. Krummheuer, V. M. Axt, and T. Kuhn, *Phys. Rev. B* **65**, 195313 (2002).
  - <sup>18</sup> A. Vagov, V. M. Axt, and T. Kuhn, *Phys. Rev. B* **66**, 165312 (2002).
  - <sup>19</sup> A. Vagov, V. M. Axt, and T. Kuhn, *Phys. Rev. B* **67**, 115338 (2003).
  - <sup>20</sup> L. Jacak, P. Machnikowski, J. Krasnyj, and P. Zoller, *Eur. Phys. J. D* **22**, 319 (2003).
  - <sup>21</sup> J. Förstner, C. Weber, J. Danckwerts, and A. Knorr, *Phys. Rev. Lett.* **91**, 127401 (2003).
  - <sup>22</sup> P. Machnikowski and L. Jacak, *Phys. Rev. B* **69**, 193302 (2004).
  - <sup>23</sup> P. Borri, W. Langbein, S. Schneider, U. Woggon, R. L. Sellin, D. Ouyang, and D. Bimberg, *Phys. Rev. Lett.* **87**, 157401 (2001).
  - <sup>24</sup> A. Vagov, V. M. Axt, T. Kuhn, W. Langbein, P. Borri, and U. Woggon, *Phys. Rev. B* **70** 201305(R) (2004).
  - <sup>25</sup> E. Biolatti, R. C. Iotti, P. Zanardi, and F. Rossi, *Phys. Rev. Lett.* **85**, 5647 (2000).
  - <sup>26</sup> S. De Rinaldis, I. D'Amico, E. Biolatti, R. Rinaldi, R. Cingolani, and F. Rossi, *Phys. Rev. B* **65**, 081309 (2002).
  - <sup>27</sup> R. Alicki, M. Horodecki, P. Horodecki, R. Horodecki, L. Jacak, and P. Machnikowski, *Phys. Rev. A* **70**, 010501(R) (2004).
  - <sup>28</sup> G. D. Mahan, *Many-Particle Physics* (Kluwer, New York, 2000).
  - <sup>29</sup> S. Adachi, *J. Appl. Phys.* **58**, R1 (1985).
  - <sup>30</sup> D. Strauch and B. Dorner, *J. Phys: Cond. Matt.* **2**, 1457 (1990).
  - <sup>31</sup> P. Borri, W. Langbein, U. Woggon, M. Schwab, M. Bayer, S. Fafard, Z. Wasilewski, and P. Hawrylak, *Phys. Rev. Lett.* **91**, 267401 (2003).
  - <sup>32</sup> U. Hohenester and G. Stadler, *Phys. Rev. Lett.* **92**, 196801 (2004).
  - <sup>33</sup> C. Cohen-Tannoudji, J. Dupont-Roc, and G. Grynberg, *Atom-Phonon Interactions* (Wiley-Interscience, New York, 1998).
  - <sup>34</sup> A. Grodecka, L. Jacak, P. Machnikowski, and K. Roszak, cond-mat/0404364; in press (unpublished).
  - <sup>35</sup> D. Birkedal, K. Leosson, and J. M. Hvam, *Phys. Rev. Lett.* **87**, 227401 (2001).
  - <sup>36</sup> P. Machnikowski and L. Jacak, *Semicond. Sci. Technol.* **19**, S299 (2004).
  - <sup>37</sup> V. M. Fomin, V. N. Gladilin, J. T. Devreese, E. P. Pokatilov, S. N. Balaban, and S. N. Klimin, *Phys. Rev. B* **57**, 2415 (1998).
  - <sup>38</sup> We used the standard multi-dimensional optimization procedure from the IMSL library.